Turkish Journal of Electrical Engineering & Computer Sciences

http://journals.tubitak.gov.tr/elektrik/

Research Article

Turk J Elec Eng & Comp Sci
(2017) 25: 1773 – 1783

doi:10.3906/elk-1602-265

Regional ionospheric trend statistics: IONOLAB-PDF

Ozan KÖROĞLU*, Feza ARIKAN
Department of Electrical and Electronics Engineering, Faculty of Engineering, Hacettepe University, Ankara, Turkey

Received: 19.02.2016 • **Accepted/Published Online:** 22.06.2016 • **Final Version:** 29.05.2017

Abstract: The ionosphere plays an important role for HF bands, space-based positioning systems, satellite communication, and propagation. The variability of the ionosphere has a complex spatiotemporal characteristic, which depends on statistical parameters. Total electron content (TEC) is one of the major observables for investigating and determining this variability. In this study, spatiotemporal within-the-hour statistical characteristics of TEC are determined for Turkey, which is located in midlatitude, using the TEC estimates from the Turkish National Permanent GPS Network-Active between the years 2009 and 2012. The TEC values have strong hourly, seasonal, and positional dependence on east-west direction, and the trend shifts according to sunrise and sunset hours. It is observed that TEC is distributed predominantly as lognormal and Weibull probability density functions (pdf). Within-the-hour pdf estimates are grouped into ionospheric seasons such as March equinox, summer, winter, and September equinox. In winter and summer seasons lognormal and during equinox seasons Weibull distributions are observed more frequently. For spatial analysis, all TEC values within the same hour and in the same region are combined in order to improve the reliability and accuracy of pdf estimates. Statistical characterization of TEC over Turkey will contribute to developing a regional and seasonal random field model, which will be used in HF channel characterization and space weather risk analysis.

Key words: Propagation, communication, ionosphere, total electron content

1. Introduction

The ionosphere is one of the atmospheric layers extending from 60 to 1000 km in altitude and consisting of ionized gases. This ionized structure of the plasma layer is mostly due to solar radiation and geomagnetic effects [1]. The ionosphere is the main contributor to the space weather, and thus a wide range of operations from HF communications to space-based positioning and navigation have to take the ionospheric variability into account. The ionosphere has a spatiotemporal varying and dispersive structure whose properties affect the signals by attenuation, frequency shift and phase rotation, absorption, and time delay. This structure depends on a very large number of parameters that have almost statistical behavior. Therefore, the determination of statistical properties of this layer is very important.

There have been various efforts in the literature to characterize the variability of the ionosphere through critical parameters of the maximum ionization layer F2, which has been summarized in [2,3]. One of the most informative studies on spatiotemporal characteristics of ionospheric parameters can be found in [4]. Averages and standard deviations of critical layer parameters are investigated with respect to high and low geomagnetic variability for high-latitude, midlatitude, and equatorial regions using the data collected from more than 100 ionosonde stations during the years 1967–1989.

*Correspondence: okoroglu@hacettepe.edu.tr

Due to the sparsity of measurements of critical layer parameters extracted from ionosondes, the total electron content (TEC) that can be estimated from dual-frequency Global Positioning System (GPS) receiver recordings [1,5,6] has been utilized to investigate the statistical nature of the ionosphere. TEC can be defined as the total number of free electrons enclosed by a 1 m^2 cross-sectional cylinder in the local zenith direction.

In [7] the location, occurrence time, and strength of the equatorial ionization anomaly (EIA) crest in the Asian-Australian region during 1996–2004 is investigated using GPS-TEC. The seasonal and positional dependence of the EIA is characterized by monthly median values during local noon. It is observed that diurnal and seasonal ionospheric variations, especially during winter anomaly, are highly complicated and one model cannot be sufficient to characterize all types of variability of the ionosphere. From the above investigations it can be observed that the ionosphere has certain temporal trends such as diurnal, seasonal, annual, and 11-year solar cycle, which also show variability with respect to high-latitude, midlatitude, and equatorial regions. The statistical investigation methods of TEC variability in the above-mentioned studies are not appropriate for incorporating the ionospheric variability in the form of channel or propagation path modeling studies. Typically, in communication channel characterization the channel statistics are represented with stationarity periods, coherence bandwidths, and probability density functions.

In the literature there have been various efforts to model the statistical structure of geophysical signals as a 'random field' [8,9]. Specifically, in [10,12] (and the references therein) the spatiotemporal variability of GPS-TEC is represented as random field Z, which comprises a slowly varying trend structure in space and time μ with added secondary variability Y as:

$$Z(\vec{r};t) = \mu(\vec{r};t) + Y(\vec{r};t) \tag{1}$$

where $\vec{r}$ is the position vector and t denotes time. In order to obtain a channel representation over Turkey, the IONOLAB group has started investigations to bring these communities together (www.ionolab.org). The first attempt is to obtain a statistical representation of the 'trend' structure of random field μ. As shown in the above studies, the trend of an ionosphere is a slowly varying function of space and time.

For temporal characterization of the trend structure of GPS-TEC, a wide sense stationarity period is determined in [12,13]. The variability of a single station can change significantly in 5 to 12 min, representing the temporal variability during disturbed and nondisturbed ionosphere in midlatitude regions. In [14], the wide sense stationarity period is investigated regionally, and the temporal update period for a TEC map is optimized according to the state of the ionosphere. In [11,15,16], it is determined that the correlation distance of midlatitude ionosphere can range from 80 to 150 km.

The first study that captured the spatiotemporal variability using a parametric probability density function (pdf) fitted to histograms of GPS-TEC by the IONOLAB group is given in [2]. In this study, it is observed that Weibull and lognormal distributions can be used to characterize within-the-hour variability of GPS-TEC. The most dominant temporal period of ionization is the diurnal cycle of 24 h. The within-the-hour variability can change from hour to hour representing this strong diurnal trend. Typically, ionization of the plasma layer increases with local sunrise and tends to decrease with local sunset. The ionization reaches its maximum value around local noon. In [3] it has been demonstrated that yearly, within-the-hour parametric pdf estimates of GPS-TEC can be grouped into representative distributions for high-latitude, midlatitude, and equatorial regions within 10° latitude separations.

In [17] within-the-hour parametric pdfs of GPS-TEC are estimated for the Turkish National Permanent GPS Network (TNPGN-Active), and it is shown that a seasonal dependence can be observed in [18]. It is

observed that TEC values have a strong hourly, seasonal, and positional dependence on east-west direction, and the growing trend shifts according to sunrise and sunset times. Also, the data are distributed predominantly as lognormal and Weibull pdf. In winter and summer seasons, lognormal distribution is observed. During equinox seasons, Weibull distribution is observed more frequently. The parametric pdf estimates are generally Weibull distributed for years with high solar activity, and for the hours of sunrise and sunset. Night and day hours are lognormal distributed, especially for low solar activity years.

In this study, within-the-hour GPS-TEC from the TNPGN-Active network between 2009 and 2012 are grouped into yearly and seasonal sets, and parametric pdfs are obtained. It is observed that the estimated pdfs show similarity in terms of distribution and parameter value for stations within $2^\circ \times 3^\circ$ in latitude and longitude, respectively. Therefore, greater Turkey is further divided into subregions of size $2^\circ \times 3^\circ$. Then the within-the-hour GPS-TEC from each station in each subregion is grouped into yearly and seasonal sets. For Turkey, which lies in the midlatitude region, four distinct seasons of ionosphere, namely winter, summer, March equinox, and September equinox, are identified. The parametric pdf estimates of TEC for each subregion, year, season, and hour are computed to characterize the variability in the spatiotemporal trend. It is observed that the within-the-hour pdf estimates for each subregion, year, and season are mostly lognormal distributed. Variability increases towards solar maximum years and for the hours of sunrise and sunset. The averages and standard deviations of the chosen distributions follow the trends in 24-h diurnal and 11-year solar cycle periods. The pdf estimates will form the basis for studies in HF channel characterization, development of a regional and seasonal random field model and threat analysis, and ionospheric correction for augmentation systems over Turkey. The computation of within-the-hour pdf is summarized in Section 2 and results are provided in Section 3.

2. Computation of spatiotemporal within-the-hour PDF of TEC

Pdfs are widely used for determining statistics of physical data [19]. Spatiotemporal variation of TEC can be characterized by observing its pdf [3,18]. In this study, TEC estimates are defined using the notation $x_{u;y;d;h}$ for a given GPS station u, year y, day d, and hour h in Eq. (2) as [2,3,17]:

$$x_{u;y;d;h} = \left[x_{u;y;d;h}\left(1\right) \cdots x_{u;y;d;h}\left(n_s\right) \cdots x_{u;y;d;h}\left(N_s\right)\right]^T \tag{2}$$

where N_s defines the number of estimate samples, and superscript T denotes the transpose operator. The TEC values, which are used for within-the-hour pdf estimations of a given GPS station u, year y, season S, and hour h, for a number of days N_d in that season are defined in Eq. (3) as:

$$x_{u;y;S;h} = \left[x_{u;y;S;d;h} \cdots x_{u;y;S;n_d;h} \ldots x_{u;y;S;N_d;h}\right]_{N_m \times 1} \tag{3}$$

where $N_m = N_d N_s$. For a subregion R, all GPS station data in year y, season S, and hour h are grouped to form the data sets:

$$x_{R;y;S;h} = \left[x_{u_1;y;S;d;h} \cdots x_{u_{n_u};y;S;n_d;h} \ldots x_{u_{N_u};y;S;N_d;h}\right] \tag{4}$$

In Eq. (4), $x_{R;y;S;h}$ represents all the TEC values of year y, season S, and hour h, which are combined together for N_u number of GPS stations in subregion R. These data sets are formed for each subregion, year, season, and hour of interest and parametric pdf estimates are obtained from histograms in a manner similar to those given in [2,3,17]. In [2,3,17,18] the investigation for the best fitting pdf for yearly and hourly TEC for one GPS station has been done over Rayleigh amplitude, Rayleigh power, lognormal, Weibull, and K-distributions. It is observed that the parametric pdf estimates of yearly and hourly GPS-TEC are predominantly lognormal and Weibull.

Therefore, in this study only lognormal and Weibull distributions are considered to be the best candidates for regional-seasonal and hourly pdf estimates of TEC. The pdf for lognormal and Weibull distributions are provided in Eqs. (5) and (6), respectively, as in [19]:

$$p_L\left(x;\underline{\theta}_L\right) = \frac{1}{x(\pi\alpha_L)^{1/2}} exp?(-\frac{(\ln x - m_L)^2}{\alpha_L}) \tag{5}$$

$$p_W\left(x;\underline{\theta}_W\right) = m_W \frac{x^{m_W-1}}{\alpha_W} exp?(-\frac{x^{m_W}}{\alpha_W}) \tag{6}$$

where $\underline{\theta}_L = [m_L\, \alpha_L]$ and $\underline{\theta}_W = [m_W\, \alpha_W]$ denote the parameter sets for lognormal and Weibull distributions, respectively. The estimates of these parameter sets from the data in the maximum likelihood (ML) sense are detailed in [2,3,17]. The estimated parameters from the data sets are defined as $\hat{\underline{\theta}}_{L_{R;y;S;h}}$ for the lognormal distribution, and $\hat{\underline{\theta}}_{W_{R;y;S;h}}$ for the Weibull distribution. In order to choose the best fitting parametric pdf to the experimental pdf, the ML ratio test detailed in [2,3,17,18] is used. For a quick reminder, the ML ratio test between lognormal and Weibull distributions is given in Eq. (7) below:

$$MLR_{R;y;S;h} = \frac{\prod_{n=1}^{N_m N_u} p_W\left(x_{R;y;S;h}(n);\hat{\underline{\theta}}_{W_{R;y;S;h}}\right)}{\prod_{n=1}^{N_m N_u} p_L\left(x_{R;y;S;h}(n);\hat{\underline{\theta}}_{L_{R;y;S;h}}\right)} \tag{7}$$

In Eq. (7), if $MLR_{R;y;S;h} > 1$ for a subregion R, year y, season S, and hour h, then the decision for the best fitting parametric pdf is chosen to be Weibull. If the ratio is smaller than 1, then the lognormal distribution is chosen. If the ratio is very close to 1, in order to decide the best fitting distribution the symmetric Kullback–Leibler distance (SKLD) between the parametric pdf and experimental pdf is calculated as discussed in detail in [17]. The parametric distribution with lower SKLD is chosen as the optimum fit for the experimental pdf. The mean and standard deviation of the lognormal distribution are provided in Eqs. (8) and (9), respectively, as:

$$\hat{\eta}_L = exp?(\hat{m}_L + \hat{\alpha}_L/4) \tag{8}$$

$$\hat{\zeta}_L = \sqrt{exp?(\hat{\alpha}_L/2 - 1)exp?(2\hat{m}_L + \hat{\alpha}_L/2)} \tag{9}$$

Similarly, the mean and standard deviation of the Weibull distribution are given in Eqs. (10) and (11), respectively, as:

$$\hat{\eta}_W = \hat{m}_W^{1/\hat{\alpha}_W}\Gamma(1 + 1/\hat{\alpha}_W) \tag{10}$$

$$\hat{\zeta}_W = \sqrt{\hat{m}_W^{2/\hat{\alpha}_W}\left(\Gamma\left(1 + 2/\hat{\alpha}_W\right) - \Gamma^2(1 + 1/\hat{\alpha}_W)\right)} \tag{11}$$

where $\Gamma(\cdot)$ denotes the gamma function. The estimated parametric pdfs for a midlatitude GPS network are demonstrated in the following section.

3. Results

In this study, the spatiotemporal pdf for GPS-TEC estimates is computed for a midlatitude region, namely Turkey, according to the method described in Section 2. The TNPGN-Active consists of 146 homogeneously distributed GPS stations, approximately 80 to 120 km apart, as shown in Figure 1 [12,17]. According to previous studies in [17,18], an optimum subregion size of $2^\circ \times 3^\circ$ is chosen in latitude and longitude, respectively. The subregions are denoted with R in Figure 1 with dashed lines. The stations, which are on the border of two subregions, are included in both subregions. The Receiver Independent Exchange (RINEX) data for the TNPGN-Active GPS network is processed with the Reg-Est algorithm as discussed in [1,6,20]. IONOLAB-TEC estimates using IONOLAB-BIAS were computed between May 2009 and September 2012 [21,22]. It has been observed in [17] that the data set can be highly sparse for some stations. Therefore, the spatiotemporal interpolation method introduced in [12] was applied to improve the statistical reliability of the data set. In [18], midlatitude ionosphere was investigated in four distinct seasons for the northern hemisphere. These seasons can be given as:

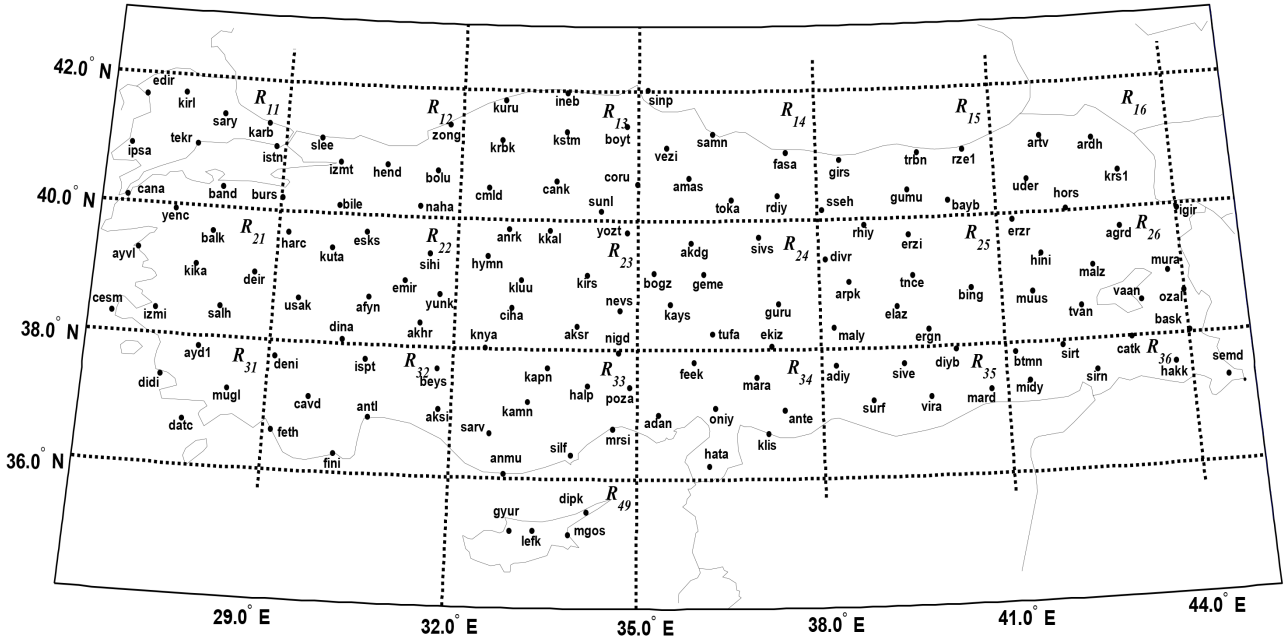

Figure 1. TNPGN-Active GPS Network, where the subregions R_{11} to R_{49} are indicated with dotted lines.

- S_1: Vernal (spring) Equinox (March, April)
- S_2: Summer (May, June, July, August)
- S_3: Autumnal Equinox (September, October)
- S_4: Winter (November, December, January, February)

and significant seasonal variability is observed in hourly TEC pdf estimates. The statistical analysis discussed in this study is applied to TNPGN-Active data between 2009 and 2012. This time interval lies within Solar Cycle 24. The solar activity started later than expected due to the anomalous solar cycle. A significant increase in TEC estimates is observed from 2009 to 2012, which is the solar maximum year.

The data sets for statistical analysis are prepared by grouping IONOLAB-TEC values for each TNPGN-Active station into yearly, seasonal, and hourly data sets, as described in Eqs. (2) and (3). An example is given in Figures 2a–2p for istn ([40.99°N, 28.83°E] in R_{12}), izmt ([40.80°N, 29.95°E] in R_{12}), and arpk ([39.04°N, 38.49°E] in R_{25}) stations. The IONOLAB-TEC estimates for istn, izmt, and arpk for the year 2010 are given in

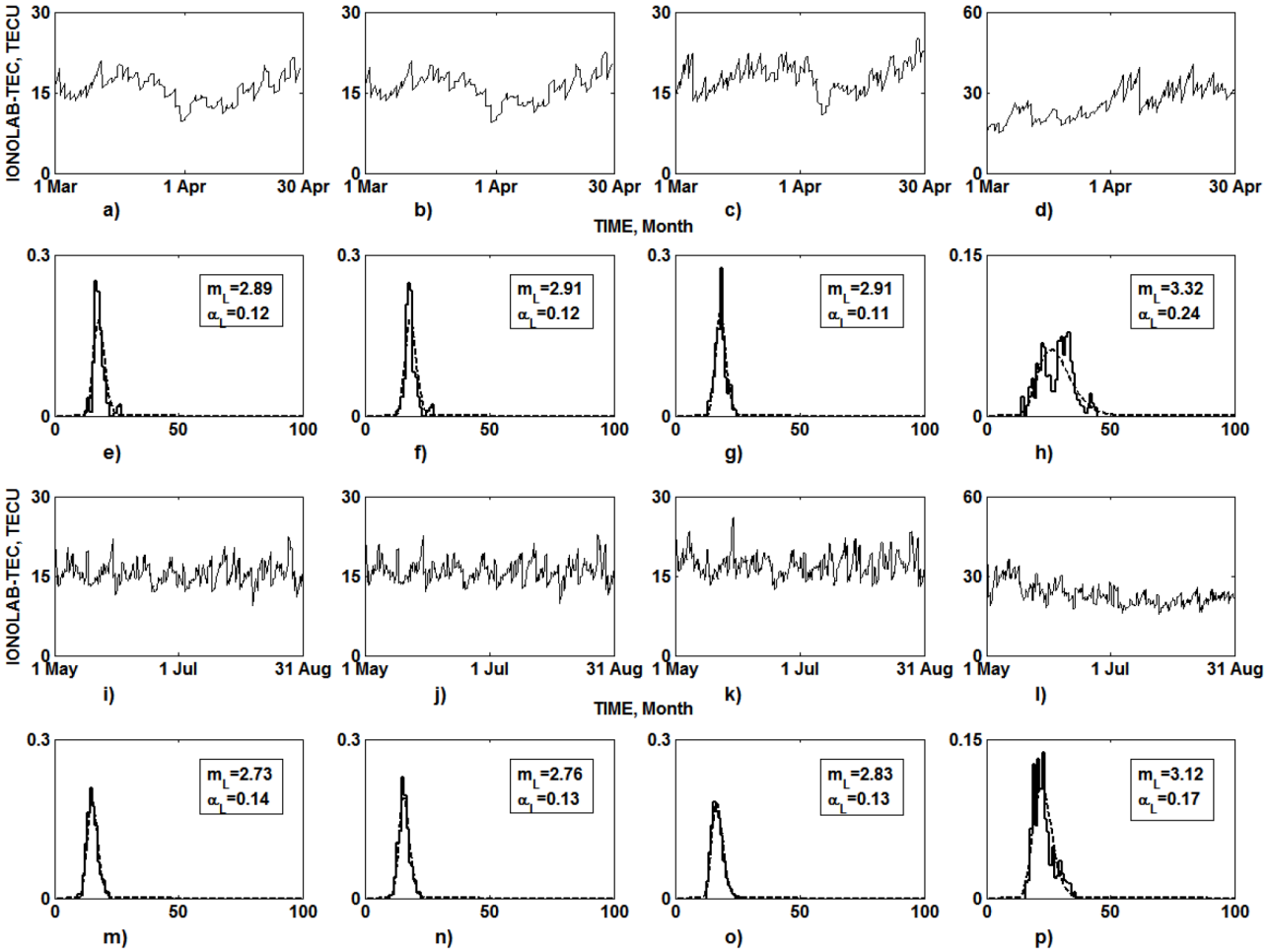

Figure 2. IONOLAB-TEC estimates: a) istn, 2010, R_1, 07000800 UTC; b) izmt, 2010, S_1, 07000800 UTC; c) arpk, 2010, S_1, 07000800 UTC; d) arpk, 2011, S_1, 07000800 UTC, parametric (dashed line) and experimental (solid line) pdf estimates; e) istn, 2010, S_1, 07000800 UTC; f) izmt, 2010, S_1, 07000800 UTC; g) arpk, 2010, S_1, 07000800 UTC; h) arpk, 2011, S_1, 07000800 UTC, IONOLAB-TEC estimates; i) istn, 2010, S_2, 07000800 UTC; j) izmt, 2010, S_2, 07000800 UTC; k) arpk, 2010, S_2, 07000800 UTC; l) arpk, 2011, S_2, 07000800 UTC, parametric (dashed line) and experimental (solid line) pdf estimates; m) istn, 2010, S_2, 07000800 UTC; n) izmt, 2010, S_2, 07000800 UTC; o) arpk, 2010, S_2, 07000800 UTC; p) arpk, 2011, S_2, 07000800 UTC.

Figures 2a, 2b, and 2c; IONOLAB-TEC for 2010, season S_1 and 0700–0800 UTC are given for stations istn, izmt, and arpk, respectively. The similarity between istn and izmt stations, which are both in region R_{12}, is highly apparent. On the other hand, $x_{arpk;2010;S_1;7}$, given in Figure 2c, is different from those in Figures 2a and 2b, since it is located in R_{25}. In Figure 2d, the TEC values are presented for $x_{arpk;2011;S_1;7}$ and the effect

of solar activity on both magnitude of TEC and variability can be observed in the comparison of Figures 2a and 2d. In Figures 2e, 2f, and 2g, a parametric pdf and its ML sense estimated parameters $\hat{\underline{\theta}}_L = [\hat{m}_L \; \hat{\alpha}_L]$ are presented for istn, izmt, and arpk stations for year 2010, season S_1, and hour 0700–0800 UTC, respectively. The parameter and pdf estimates of the istn, izmt, and arpk data sets are found to be lognormal. The data histograms and parametric pdf estimates are given in dashed and solid lines, respectively.

In Figures 2i, 2j, and 2k IONOLAB-TEC for 2010, season S_2, and 0700–0800 UTC are given for stations istn, izmt, and arpk, respectively. The similarity seen in season S_1 is valid for season S_2. The istn and izmt stations' behavior is similar, as both are in region R_{12}. On the other hand, $x_{arpk;2010;S_2;7}$, given in Figure 2k, is different from those in Figures 2i and 2j, since it is located in R_{25}. Figure 2l shows $x_{arpk;2011;S_2;7}$ and the effect of solar activity on both magnitude of TEC and variability can be observed in the comparison of Figures 2a and Figure 2d. In Figures 2m–2o the pdf estimates of istn, izmt, and arpk are given for the year 2010, hour 0700–0800 UTC, but this time season S_2 is chosen. The pdf estimates are all lognormal with similar parameters. In Figure 2p, the arpk station, year 2011, hour 0700–0800, and S_2 season pdf estimate is indicated. The estimate is lognormal with parameters slightly different from those found in Figures 2m–2o. The IONOLAB-TEC examples provided in Figure 2 indicate the variation between subregional, yearly, seasonal, and hourly TEC values. Figure 2 also provides a clear indication that pdf estimates from stations from the same subregion, same year, same season, and same hour interval are similarly distributed. Therefore, the data sets from the GPS stations in the same subregion can be combined to form one large set, which will improve the statistical reliability.

In order to obtain spatiotemporal TEC distributions the IONOLAB-TEC data for each station, year, season, and hour are grouped into subregional sets $x_{R;y;S;h}$, as described in Eq. (4). The pdf and parameter estimation method used in [2,3,17,18] is applied to $x_{R;y;S;h}$ in the ML sense. The best fitting pdf distribution is obtained using Eq. (7). It is observed that subregional, yearly, seasonal, and hourly pdf estimates differ from each other significantly both in parameter value and distribution. An example is provided in Figures 3a–3p for subregions R_{12} and R_{25}, years 2010 and 2011, seasons S_1 and S_2, and hours 0700–0800 UTC and 1400–1500 UTC. In Figure 3 the experimental pdfs (histograms) are given in solid lines and parametric pdf estimates are indicated with dashed lines.

Figures 3a and 3b are plots of the IONOLAB-TEC values from 2010 for region R_{12}, season S_1, at 0700–0800 UTC and 1400–1500 UTC, respectively. The variation depending on hour interval can be seen from these two subfigures. The experimental pdfs and parametric pdf estimates of these two hour intervals are provided in Figures 3e and 3f, respectively. The parametric pdf estimates for 2010, region R_{12}, and season S_1 at 0700–0800 UTC and at 1400–1500 UTC are both lognormal with parameter estimates very close to each other.

When Figure 3c is compared to Figure 3a, the seasonal variation in TEC can be easily observed for the same region, same year, and same hour. As a consequence, the experimental and parametric pdfs given in Figures 3g and 3e are also different.

In Figure 3d, IONOLAB-TEC values of region R_{12} for 2011, season S_1 at 0700–0800 UTC are provided. When compared to those in Figure 3a, the variability in magnitude and distribution of TEC with respect to year is apparent. As a result, the experimental and parametric pdfs provided in Figure 3h, although lognormally distributed, differ significantly from those given in Figure 3e in terms of estimated parameters $\hat{m}_L$ and $\hat{\alpha}_L$.

Figures 3i and 3j are the plots of the IONOLAB-TEC values from 2010 for region R_{25}, season S_1 at 0700–0800 UTC and 1400–1500 UTC, respectively. The variation depending on hour interval can be seen from these two subfigures. The experimental pdfs and parametric pdf estimates of these two hour intervals are

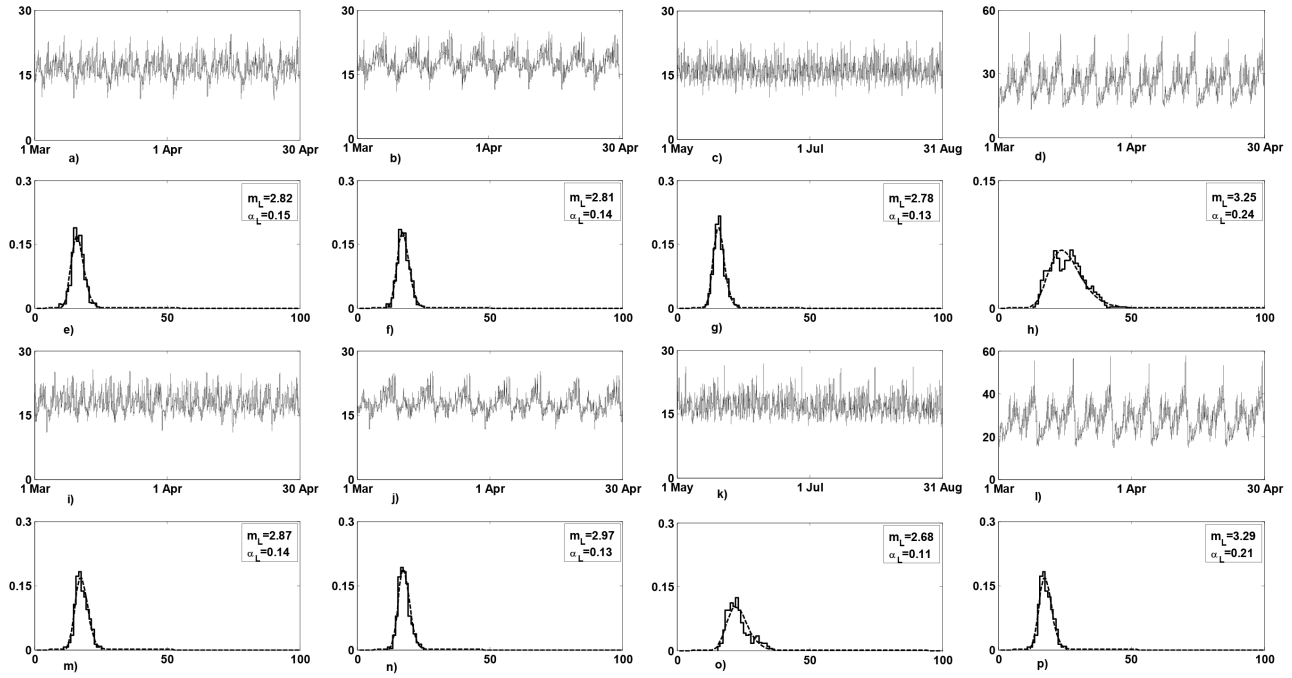

Figure 3. IONOLAB-TEC estimates: a) S_1, R_{12}, 2010, 07000800 UTC; b) S_1, R_{12}, 2010, 14001500 UTC; c) R_2, R_{12}, 2010, 07000800 UTC; d) R_1, R_{12}, 2011, 07000800 UTC, parametric (dashed line) and experimental (solid line) pdf estimates; e) R_1, R_{12}, 2010, 07000800 UTC; f) R_1, R_{12}, 2010, 14001500 UTC; g) R_2, R_{12}, 2010, 07000800 UTC; h) R_1, R_{12}, 2011, 07000800 UTC, IONOLAB-TEC estimates; i) R_1, R_{25}, 2010, 07000800 UTC; j) R_1, R_{25}, 2010, 14001500 UTC; k) R_2, R_{25}, 2010, 07000800 UTC; l) S_1, R_{25}, 2011, 07000800 UTC, parametric (dashed line) and experimental (solid line) pdf estimates; m) S_1, R_{25}, 2010, 07000800 UTC; n) S_1, R_{25}, 2010, 14001500 UTC; o) R_2, R_{25}, 2010, 07000800 UTC; p) R_1, R_{25}, 2011, 07000800 UTC.

provided in Figures 3m and 3n, respectively. The parametric pdf estimates for 2010, region R_{25} and season S_1 at 0700–0800 UTC and at 1400–1500 UTC, are both lognormal with parameter estimates very close to each other. When Figure 3k is compared to Figure 3i, the seasonal variation in TEC can be easily observed for same region, same year, and same hour. Consequently, the experimental and parametric pdfs given in Figure 3o are also different from those in Figure 3g. The regional variation can be observed by comparing Figure 3c with Figure 3k, and Figure 3g with Figure 3o.

In Figure 3l the IONOLAB-TEC values of region R_{25} for 2011, season S_1 at 0700–0800 UTC, are provided. When compared to those in Figure 3i, the variability in magnitude and distribution of TEC with respect to year is apparent. As a result, the experimental and parametric pdfs provided in Figure 3p, although lognormally distributed, differ significantly from those given in Figure 3m in terms of parameters $\hat{m}_L$ and $\hat{\alpha}_L$.

In comparing these subfigures, improvement in TEC representation with regional grouping of data is apparent. The pdfs are all represented with lognormal distribution with reduced difference in terms of distribution parameters.

From the above examples, the spatiotemporal variability of TEC can be observed with respect to the subregions, years, seasons, and hours. In this study, for each year, season, and hour, both the individual pdf estimates of stations and subregional pdf estimates are computed. It is observed that there is an excellent agreement in the mean and standard deviation of pdf estimates for the stations in the subregion and subregional

pdf estimates. The purpose of dividing the data according to regional and seasonal point of view comes with an impact of improvement of the mathematical model of the ionosphere. It allows us to understand and model this variation in a probabilistic way.

In order to demonstrate this behavior, Figure 4 is presented as an example to indicate the variability for all subregions for the year 2011 and S_1 season. In the figure, Eqs. (8)–(11) are used. The mean $\hat{\eta}$ and standard deviation $\hat{\zeta}$ estimates given in Figure 4 show that there is a very good agreement with latitude and longitude variation for all regions according to their geographical location. The northern stations' mean and standard deviations are much smaller while the southern ones are higher. Also, according to sunrise times, the eastern regions see a rise in mean before the western ones.

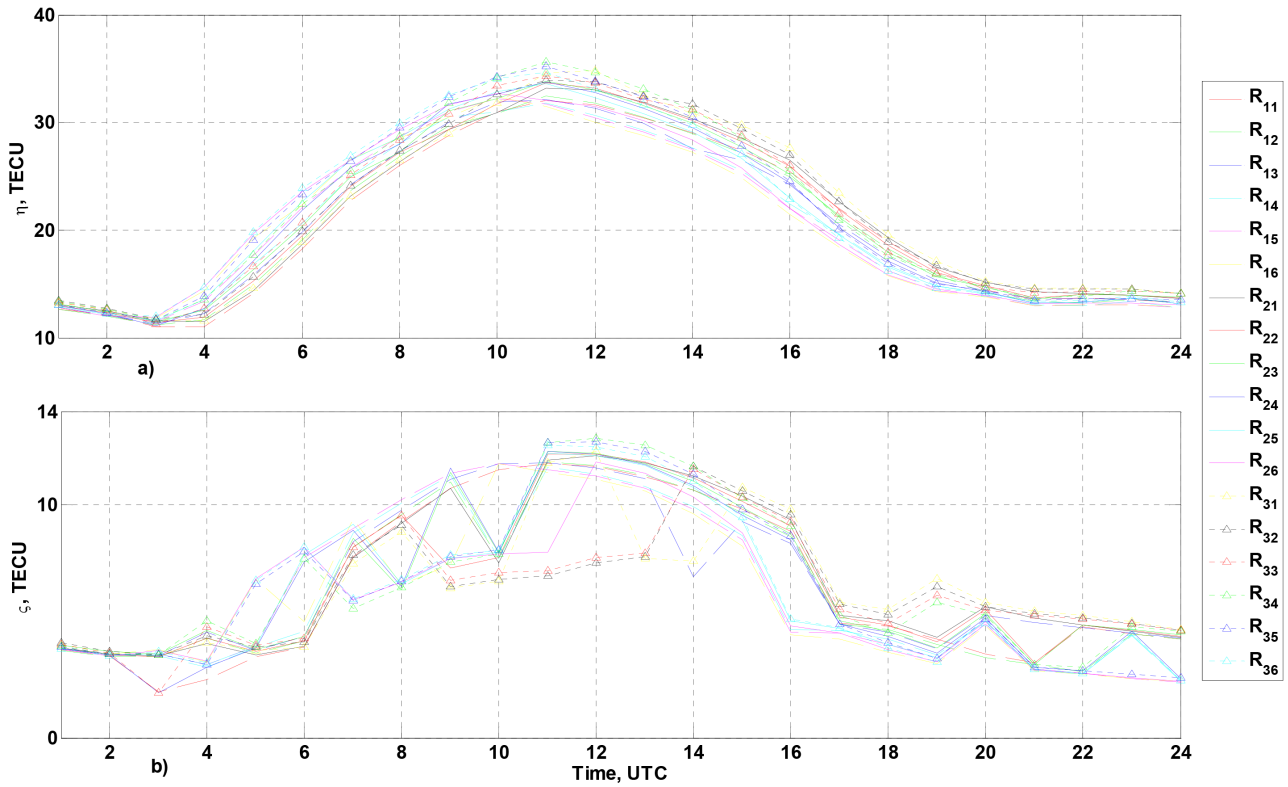

Figure 4. Mean $\hat{\eta}$ and standard deviation $\hat{\zeta}$ of subregional parametric pdfs for year 2011 and season R_1 for each subregion.

The example provided in this section demonstrates the spatiotemporal variability of TEC and importance of subregional, yearly, seasonal, and hourly statistical analysis.

4. Conclusion

The spatiotemporal variability of the TEC trend is analyzed by parametric probability density functions. The TEC values are estimated using GPS and the data are grouped spatially into subregions, and temporally as years, seasons, and hours. The two major pdfs that represent the spatiotemporal trend behavior of TEC are decided to be lognormal and Weibull distributions. The IONOLAB-PDF method is applied to the data from the midlatitude GPS network between 2009 and 2012 for the first time. It is observed that the parametric pdf estimates of

GPS-TEC are in accordance with the expectation of temporal trends in a midlatitude region. The variability of the parameters of the chosen distributions is shown to be in accordance with spatial trends of background ionosphere. Variability increases during sunrise and sunset hours, equinox seasons, and solar active years. For these hours, seasons, and years, the distribution is predominantly Weibull. Local noon and night hours, summer and winter seasons, and geomagnetically quiet periods are distributed as predominantly lognormal. The variability with respect to latitude and longitude is in agreement with the expected spatiotemporal trends of the ionosphere. The statistical analysis presented in this study forms a basis for future studies in estimation of experimental pdfs for critical parameters obtained from ionosondes, probabilistic channel characterization for HF communication links for midlatitude regions, spatiotemporal trend analysis for seasonal and hourly ionospheric anomalies, and statistical modeling of TEC over Turkey. The results of this work provide an important basis for HF communication and propagation studies.

Acknowledgments

The TNPGN-Active RINEX data set was made available to the IONOLAB group for the TÜBİTAK 109E055 project. The data set can be accessed by permission from TÜBİTAK and the General Command of Mapping of the Turkish Army (www.hgk.msb.gov.tr). This study was supported by a joint grant of TÜBİTAK, 112E568 and RFBR 13-02-91370-CT_a.

References

[1] Arikan F, Erol CB, Arikan O. Regularized estimation of vertical total electron content from Global Positioning System data. J Geophys Res-Space 2003; 108: 1469.

[2] Türel N. Power spectral density and probability density function estimation of the total electron content of the ionosphere layer. MSc, Hacettepe University, Ankara, Turkey, 2008 (in Turkish with abstract in English).

[3] Turel N, Arikan F. Probability density function estimation for characterizing hourly variability of ionospheric total electron content. Radio Sci 2010; 45: RS6016.

[4] Forbes JM, Palo SE, Zhang X. Variability of the ionosphere. J Atmos Sol-Terr Phy 2000; 62: 685-693.

[5] Komjathy A. Global ionospheric total electron content mapping using the global positioning system. PhD, University of New Brunswick, Fredericton, Canada, 1997.

[6] Nayir H, Arikan F, Arikan O, Erol CB. Total electron content estimation with Reg-Est. J Geophys Res-Space 2007; 112: A11313.

[7] Zhao B, Wan W, Liu L, Ren Z. Characteristics of the ionospheric total electron content of the equatorial ionization anomaly in the Asian-Australian region during 1996. Ann Geophys 2009; 27: 3861-3873.

[8] Vanmarcke E. Random Fields: Analysis and Synthesis. Cambridge, MA, USA: MIT Press, 1988.

[9] Cressie NAC. Statistics for Spatial Data. Revised Edition. New York, NY, USA: John Wiley and Sons, 1993.

[10] Sayın I. Total electron content mapping using kriging and random field priors. MSc, Hacettepe University, Ankara, Turkey, 2008 (in Turkish with abstract in English).

[11] Deviren MN. Estimation of space-time random field for total electron content (TEC) over Turkey. MSc, Hacettepe University, Ankara, Turkey, 2013 (in Turkish with abstract in English).

[12] Sayin I, Arikan F, Arikan O. Regional TEC mapping with random field priors and kriging. Radio Sci 2008; 43: RS5012.

[13] Erol CB, Arikan F. Statistical characterization of the ionosphere using GPS signals. J Electromagnet Wave 2005; 19: 373-387.

[14] Sayin I, Arikan F, Akdogan KE. Optimum temporal update periods for regional ionosphere monitoring. Radio Sci 2010; 45: RS6018.

[15] Karatay S. Investigation of the relationship between earthquakes and total electron content. PhD, Fırat University, Elazığ, Turkey, 2010 (in Turkish with abstract in English).

[16] Karatay S, Arikan F, Arikan O. Investigation of total electron content variability due to seismic and geomagnetic disturbances in the ionosphere. Radio Sci 2010; 45: RS5012.

[17] Köroğlu O. Statistical analysis of total electron content using TNPGN and TNPGN-active network. MSc, Hacettepe University, Ankara, Turkey, 2012 (in Turkish with abstract in English).

[18] Koroglu O, Arikan F, Deviren MN. Regional and seasonal parametric probability density function estimation for total electron content. In: 22ndSignal Processing and Communications Applications Conference; 23–25 April 2014; Trabzon, Turkey. New York, NY, USA: IEEE. pp. 915-918.

[19] Papoulis A. Probability, Random Variables and Stochastic Processes. Singapore: McGraw-Hill, 2002.

[20] Arikan F, Erol CB, Arikan O. Regularized estimation of vertical total electron content from GPS data for a desired time period. Radio Sci 2004; 39: RS6012.

[21] Sezen U, Arikan F, Arikan O, Ugurlu O, Sadeghimorad A. Online, automatic, near-real time estimation of GPS-TEC: IONOLAB-TEC. Adv Space Res 2013; 11: 297-305.

[22] Arikan F, Nayir H, Sezen U, Arikan O. Estimation of single station interfrequency receiver bias using GPS-TEC. Radio Sci 2008; 43: RS4004.